Journal of Non-Crystalline Solids 357 (2011) 2763–2768

Contents lists available at ScienceDirect

Journal of Non-Crystalline Solids

journal homepage: www.elsevier.com/ locate/ jnoncrysol

Molecular dynamics simulation of radiation damage in glasses

J.-M. Delaye [a,*], S. Peuget [a], G. Bureau [a], G. Calas [b]

[a] CEA EA Marcoule, DEN/DTCD/SECM, BP17171, 30207 Bagnols-sur-Cèze cedex, France

[b] Institut de Minéralogie et de Physique des Milieux Condensés, Université Pierre et Marie Curie, CNRS UMR 7590, Université Paris Diderot, IPGP, Case 115, 4 Place Jussieu, 75 005 Paris, France

ARTICLE INFO

Article history:
Received 10 November 2010
Received in revised form 10 February 2011
Accepted 12 February 2011
Available online 29 March 2011

Keywords:
Molecular dynamics;
Radiation effects;
Borosilicate glass;
Silica;
Glass structure

ABSTRACT

Molecular dynamics simulations of the ballistic effects arising from displacement cascades in glasses have been investigated in silica and in a SiO_2–B_2O_3–Na_2O glass. In both glasses the T-O-T′ angle (where T and T′ are network formers) diminishes, despite radiation causes opposite effects: while the ternary glass swells and silica becomes denser. We show that radiation-induced modifications of macroscopic glass properties result from structural change at medium/range, reflecting an increasing disorder and internal energy of the system. A local thermal quenching model is proposed to account for the effects of ballistic collisions. The core of a displacement cascade is heated by the passage of the projectile, then rapidly quenched, leading to a process that mimics a local thermal quenching. The observed changes in both the mechanical and structural properties of glasses eventually reach saturation at 2 10^{18} α/g as the accumulated energy increases. The passage of a single projectile is sufficient to reach the maximum degree of damage, confirming the hypothesis postulated in the swelling model proposed by J.A.C. Marples.

1. Introduction

Vitrification of high-level radioactive waste in borosilicate glasses is currently used on an industrial scale in several countries. The fundamental properties of the waste forms are their chemical and mechanical durability against the forcing conditions represented by chemical alteration or internal/external irradiation. At the molecular scale, glass structure is modified by radiation effects and by other internal (chemical composition) or external (alteration) variables [1]. Understanding the radiation effects in glasses is then an important topic to model the long term stability of nuclear waste matrices [2,3]. The effects of irradiation can be elastic (cascades of ballistic collisions between atoms) or inelastic (changes in the electronic structure associated with the formation of point defects) [4].

Recent data on active nuclear glasses indicate the predominance of ballistic effects in accounting for the macroscopic changes at doses up to 10^{19} α/g [5,6]. Under irradiation, the glass density and hardness diminish, while fracture toughness increases up to a saturation threshold. Saturation is reached for critical doses of about 2×10^{18} α/g and appears to be effective at least to a dose of 10^{19} α/g. Alkali borosilicate glasses present the same qualitative behavior as nuclear glasses under irradiation by heavy ions (inducing mainly ballistic effects), e.g. a swelling of a few percent, as shown by experiment and numerical simulation [1,7,8]. Radiation effects in silica have also been studied for years, with a noticeable densification under a very large range of irradiating fluxes : neutrons, electrons, and X-rays. [9–11]. There is then an opposite evolution of pure silica and ternary borosilicate glasses under irradiation leading to elastic effects.

The situation is rather more complicated when a mixing between the elastic and inelastic effects is considered in ternary glasses. In this case, it is possible to observe a swelling at low doses, followed by a compaction at larger doses [12]. In silica, the presence of impurities (like hydrogen) can play a major role on the density behavior [13,14]. For instance, the densification reverses to swelling when a sufficient concentration of H atoms are incorporated in the silica structure [14].

In order to identify more precisely the origin of this different behavior, we have simulated by classical molecular dynamics (MD), series of displacement cascades in amorphous silica and an alkali borosilicate glass, in order to progressively damage the bulk glass by ballistic effects. Prior studies have focused on the impact of individual different displacement cascades with different ion energies on the structure of borosilicate glasses [15,16]. Silica glass is an archetypal structure of tridimensional oxide glasses. The structure of alkali borosilicate glasses has also been extensively investigated because the mixing of Na_2O and B_2O_3 gives them original non linear properties [17–19]. The available observables provide a firm basis for numerical simulation of the structure of these glasses.

The present study shows that the structure of both a silica glass and an alkali borosilicate glass suffers an increasing structural disorder at short and medium-range distance, as well as an increase in the internal energy of the system. Ballistic effects modify glass structure, retaining the memory of a higher fictive temperature due to a fast thermal quenching. The different behavior of glass structure under irradiation is explained by the coordination change of Si and O

* Corresponding author. Tel.: +33 04 66 79 17 94; fax: +33 04 66 79 77 08.
E-mail address: jean-marc.delaye@cea.fr (J.-M. Delaye).

0022-3093/$ – see front matter © 2011 Elsevier B.V. All rights reserved.
doi:10.1016/j.jnoncrysol.2011.02.026

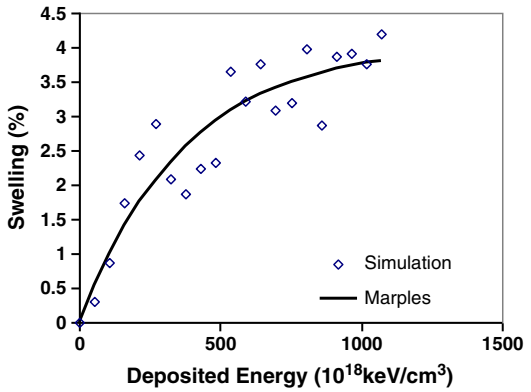

Fig. 1. Swelling of CJ1 glass versus the energy deposited by accumulating a series of 600 eV displacement cascades.

in the silica glass and of B in the borosilicate glass as a result of the migration of Na from a charge-compensating to a network modifying position.

2. Methodology

The molar composition of the borosilicate (CJ1) glass is the following: 67.7% SiO_2–18.1% B_2O_3–14.2% Na_2O. The simulation cell comprised 4000 and 3999 atoms for CJ1 and silica glass. The CJ1 glass was chosen because its behavior under irradiation shows that it is a good analog of active nuclear glasses [7,8].

The CJ1 glass was produced using the formalism described by Delaye and Ghaleb [15] by classical MD using Born–Mayer–Huggins potentials supplemented by three-body terms [20]. BKS potentials were used to simulate the structure of silica [21].

The glasses were fabricated in several steps. Initially, a liquid was equilibrated for 100,000 time steps starting from a random configuration. The volume was maintained constant. Whenever the temperature exceeded 6000 K, the atomic velocities were reequilibrated to return to 4000 K. At the end of the liquid equilibration period the glass was quenched at the rate of 5×10^{12} K/s. The temperature was lowered stepwise; and the value and duration of each temperature level were adjusted to match the quenching rate. The simulation cell volume remained constant during quenching. The equilibrium volume of the quenched glass at a room temperature was determined by calculating 20,000 time steps at constant pressure. A final relaxation for 10,000 time steps was applied at constant volume using the equilibrium volume determined during the preceding step. The glassy configurations were thus equilibrated at a room temperature and characterized by a near-zero pressure. The time step used for the glass preparation was 1 fs. During the glass fabrication, heavy atoms (with a mass equal to that of U atoms) were inserted in the structures to obtain projectiles capable of initiating the displacement cascades. To do this, 4 Si atoms are simply "modified" to attribute them the mass of a U atom. With regard to interactions, these atoms are treated like Si atoms, i.e. by application of Si-*X* potentials (where *X* is any atom). Only their mass differs from that of Si atoms.

A displacement cascade is initiated by accelerating a heavy projectile with an energy of 600 eV. The energy displacement of the cascades is adjusted so the cascade volume is contained within the simulation cell. Only a few percent of the total number of network-forming atoms are displaced during a cascade. Displacement cascades in oxide glasses are homogeneous along the initial projectile path because there is no preferred direction for the propagation of atomic displacements as in crystals, which ensures that the displacement cascades are circumscribed within the simulation cell. The energy of the initial projectile decays through a series of ballistic collisions with the atoms of the glass. Ziegler, Biersack and Littmark (ZBL) potentials are used to correctly model the high-energy interactions of the collisions [22]. These potentials are related to the pair potentials by polynomial expressions of degree 5 ensuring continuity of energy, forces, and force derivatives. A thickness of 3 Å is maintained at a room temperature around the edges of the simulation cell by regularly controlling the atomic velocities to absorb thermal motion as it reaches the edges.

All displacement cascades follow one another without changing the equilibrium volume between each cascade, resulting in a gradual increase in pressure with the deposited energy. The new equilibrium volume of the glass is then calculated throughout the NPT ensemble from the structure integrating all the displacement cascades. This method limits swelling as the dose increases. A variable time step is used in the simulation of displacement cascades. It is short at the beginning to correctly sample the paths of the highest-energy atoms, and increases as the energy decays, finally reaching 1 fs. A hysteresis system detailed in [23] is applied to modify the time step.

3. Results

3.1. Evolution of the macroscopic properties of the SiO_2–B_2O_3–Na_2O glass

The CJ1 glass subjected to a series of 600 eV displacement cascades exhibits a volume expansion shown in Fig. 1.

The shape of the swelling can be fitted to an exponential law [24]:

$$\frac{\Delta V}{V_0} = \left(\frac{\Delta V}{V}\right)_{sat}\left[1 - exp\left(-V_p D t\right)\right]. \quad (3)$$

In this equation, V_0 and ΔV correspond respectively to the initial volume and to the volume change at time *t*. $(\Delta V/V)_{sat}$ corresponds to

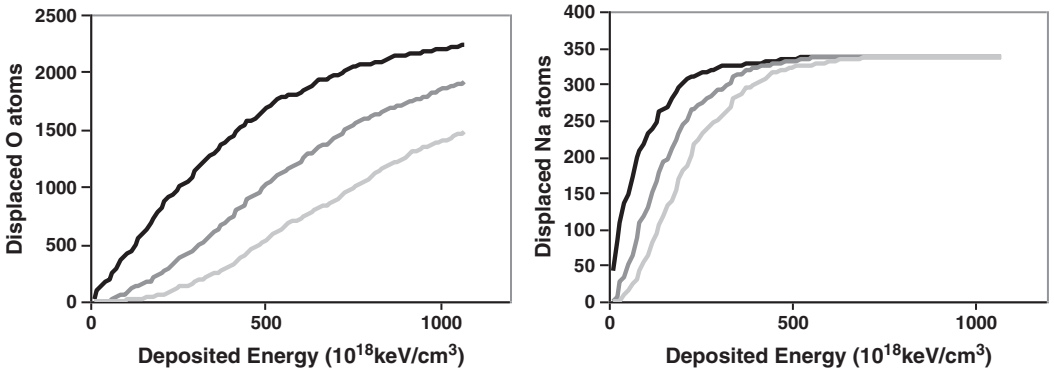

Fig. 2. Left: number of oxygen atoms displaced at least once (black), twice (dark gray) or 3 times (light gray) versus the deposited energy in a series of 600 eV displacement cascades in CJ1 glass. Right: the same thing for the Na atoms.

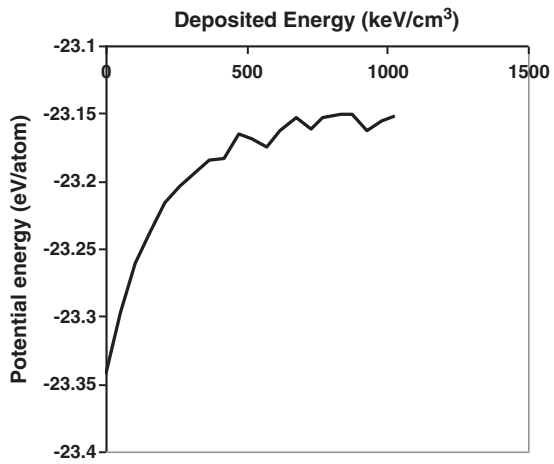

Fig. 3. Potential energy versus deposited energy during the accumulation of 600 eV displacement cascades in CJ1 glass.

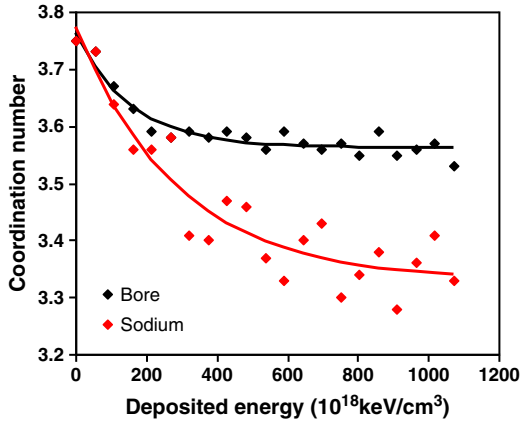

Fig. 5. Evolution of the mean coordination number of boron and sodium atoms in CJ1 glass subjected to a series of 600 eV cascades. Trend lines were fitted using exponential functions. The Na coordination is shifted to be visualized on the same scale.

the final saturation plateau. D is the dose (in particle/nm^3/s), and V_p is the elementary volume damaged by one projectile.

In establishing this relation, Marples [24] formulated the hypothesis that the passage of a single projectile is sufficient to reach a maximum damage locally. Each new projectile therefore modifies the structure only if it passes through a region that was not previously irradiated. As the probability of irradiating an untouched area diminishes as the dose increases, swelling slows down according to an exponential law. To confirm this model, we have plotted in Fig. 2 the number of oxygen atoms displaced at least once, twice or three times versus the deposited energy.

An oxygen atom is considered to be displaced if it moves over a distance exceeding 1 Å during a cascade. The curves corresponding to displacements of Si and B atoms are similar to the curve for oxygen atoms. Na atoms behave differently. They are much more mobile, and are displaced by ballistic collisions as well as under the effect of thermal motion and changes in Coulomb interactions. All the Na atoms are shifted much more rapidly than the atoms forming the glass skeleton. Swelling appears to be correlated with the number of O atoms displaced once. Both curves tend simultaneously toward the saturation threshold. This simultaneity is not observed for O atoms displaced at least two or three times. Marples' model is therefore justified. Moving each forming atom (O, Si or B) only once is enough to reach the maximum local swelling.

The variation of the potential energy in CJ1 glass due to the accumulation of displacement cascades has also been measured by quenching the glassy configurations at zero temperature to eliminate thermal motion. Fig. 3 shows the increase in potential energy with the deposited nuclear energy. A saturation threshold appears around 5×10^{20} keV/cm^3 that seems slightly lower than the saturation threshold corresponding to swelling. A similar saturation threshold has been observed during self-irradiation of Cm-bearing glasses, with saturation being attained at cumulative doses larger than 10^{17} α-decays/g [2].

The increase in potential energy reflects the evolution of the glass toward a less stable structure due to the accumulation of ballistic collisions. The high rate of glass restoration after the passage of a projectile prevents a complete medium-range reconstruction, and thus accounts for the higher potential energy. In actual nuclear glasses, a larger offset by about 1 order of magnitude is measured between the saturation times of the stored energy and of the volume expansion [2]. A much smaller lag is observed here. We currently have no explanation for this discrepancy between the experimental and simulated results.

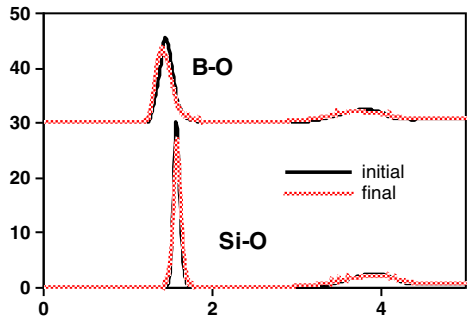

Fig. 4. Radial distribution functions for Si–O (bottom) and B–O (top) at the beginning and end of the series of 600 eV cascades in CJ1 glass. The B–O radial distribution function is offset for greater clarity.

3.2. Evolution of the structural properties of alkali borosilicate glasses

In the radial distribution function, the (Si, B)O peak decreases and broadens with glass irradiation, indicating an increasing disorder (Fig. 4). The Si–O distance does not change, as the SiO_4 tetrahedra remain stable. However, the B–O distance shifts toward smaller distances due to the ^{IV}B to ^{III}B coordination change.

The integral of the radial distribution functions up to the minimum following the first peak provides the coordination numbers. The boron coordination number decreases as a function of the deposited energy due to the increasing proportion of ^{III}B until a saturation level is reached (Fig. 5). The formation of a BO_3 entity requires fewer diffusion processes than that of a BO_4 entity. In addition, the formation of ^{III}B sites is favored at a high temperature [25], with ^{III}B–O distances shorter than ^{IV}B–O distances. This accounts for the slight shift of the first peak in the B–O radial distribution function (Fig. 4). This indicates a fast restoration of the glass structure after the passage of the projectile, keeping a memory of a higher fictive temperature of the local glass structure. The variation of the mean boron coordination number with deposited energy follows an exponential evolution, as described above for the volume expansion of the irradiated glass (Fig. 5). Experimental evidence is provided by a boron K-edge XANES

Table 1
Coordination numbers of boron atoms, and percentages of Q_n species at the beginning and end of the series of 600 eV cascades in CJ1 glass.

	$B^{[3]}$%	$B^{[4]}$%	Q_4	Q_3	Q_2	Q_1	Q_0
Initial	25%	75%	95.8%	4.2%	0%	0%	0%
Final	47%	53%	85.2%	14.6%	0.2%	0%	0%

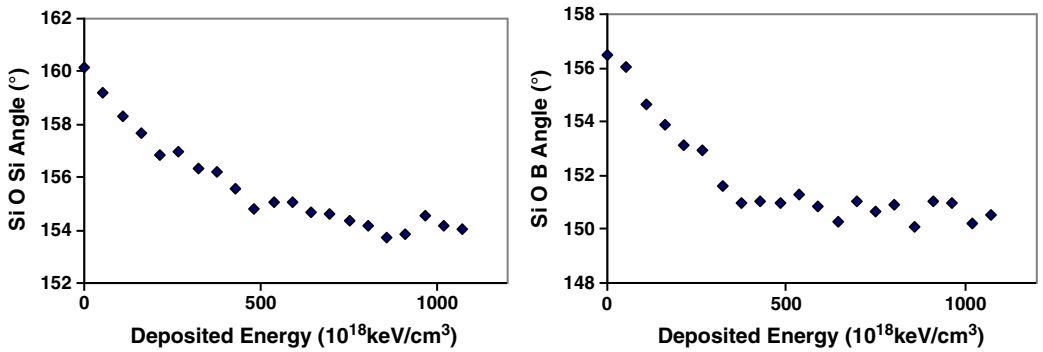

Fig. 6. Evolution of Si–O–Si and Si–O–B angles in CJ1 glass subjected to a series of 600 eV cascades.

spectroscopy of similar alkali borosilicate glasses externally irradiated by heavy ions.

The decrease of the mean boron coordination implies a modification of the role of sodium:

$$BO_4^- + Na^+_{\text{charge comp.}} \leftrightarrow BO_3 + O_{nb} + Na^+_{\text{modif.}}$$

in which $Na^+_{\text{charge comp}}$ and Na^+_{modif} represent Na^+ ions in a network-modifying and charge-compensating position. Since a network-modifying Na atom is closer to an oxygen atom than a charge-compensating Na and its coordination number is lower, we observe not only a decrease in the mean coordination number of sodium atoms but also a shift toward smaller distances for the first peak in the Na-O radial distribution function.

Nonbridging oxygen atoms are formed, modifying the degree of cross-linking around Si atoms. Table 1 indicates the coordination numbers of the boron atoms, as well as the percentages of Q_n groups at the beginning and end of the series of 600 eV displacement cascades in CJ1 glass. Q_n refers to a SiO_4 entity with n bridging oxygen atoms, and thus $(4-n)$ nonbridging oxygens.

The decrease in the mean coordination number of boron is correlated with the formation of Q_3 species and, to a lesser extent, of Q_2 species. The mean Si–O–Si and Si–O–B angles diminish under irradiation as shown in Fig. 6. The decrease in the mean angles reaches a saturation threshold matching that of the swelling and of the other structural properties.

A similar decrease with the dose is observed for the mean ring size in CJ1 glass, with a broadening of the ring size distribution. Fig. 7 compares the ring size distributions before and after the accumulation of 600 eV cascades in CJ1 glass. We considered here the rings formed by the formers Si and B connected by the O atoms. The broader distribution and the shift toward a smaller mean ring size are clearly visible. As for the angles, these phenomena reflect an increasing degree of disorder in the glass.

These phenomena – smaller angles and broader ring size distribution – have already been identified [26] due to the acceleration of thermal quenching during the fabrication of the glass. Increasing the glass thermal quenching rate generally leads to changes qualitatively equivalent to the effects of irradiation [27,28]. Experimentally, the reduction of the Si–O–Si angles was demonstrated by a Raman spectroscopy in a glass of the same composition externally irradiated by heavy ions [7]. The shift of the 500 cm^{-1} band toward higher wave numbers was interpreted as a decrease in the Si–O–Si angle. In our case the displacement cascades have a role comparable to an acceleration of the quenching rate, because, after the passage of the projectile the irradiated volume is quickly quenched to a room temperature, thus preventing any medium-range relaxation of the glass structure.

3.3. Evolution of the structural properties of silica

Amorphous silica densifies as ballistic collisions accumulate (see Fig. 8), reaching a saturation threshold of 3.5%. A similar densification was observed experimentally in silica samples irradiated by neutrons [9,10]. As the glass density, the internal energy increases up to a saturation level (Fig. 9). The saturation of the increase of the potential energy occurs simultaneously with that of the swelling. We have plotted the variation of the Si and O coordination numbers during the accumulation of displacement cascades in Fig. 10. ^{V}Si and a few ^{VI}Si appear under irradiation. Oxygen triclusters form to compensate the charge of the new entities. As for CJ1 glass, the Si–O–Si angle diminishes with the accumulation of displacement cascades (Fig. 11). The decrease of about 8° is slightly higher than in the CJ1 glass and is consistent with experimental observations in irradiated silica [10]. Ring size distribution is broader as the deposited energy increases, as the mean ring size decreases with a maximum probability diminishing from 5 to 4. (Fig. 12). The increasing disorder in the silica is also

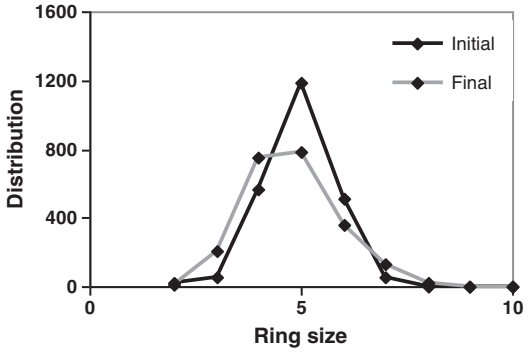

Fig. 7. Ring size distribution at the beginning and end of the accumulation of a series of 600 eV cascades in CJ1 glass.

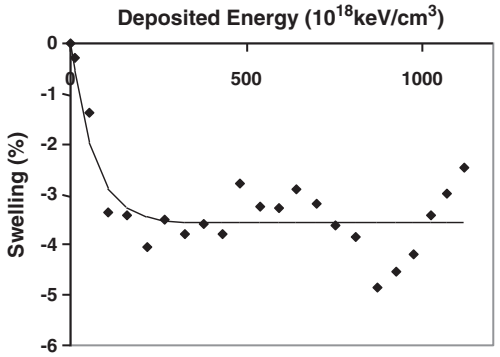

Fig. 8. Silica densification with the accumulation of 600 eV displacement cascades.

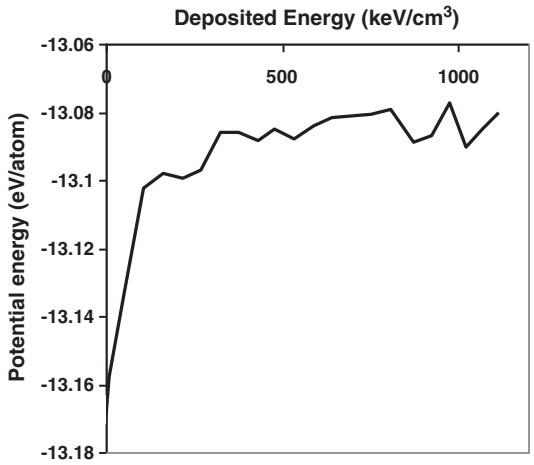

Fig. 9. Potential energy versus deposited energy during the accumulation of 600 eV displacement cascades in silica glass.

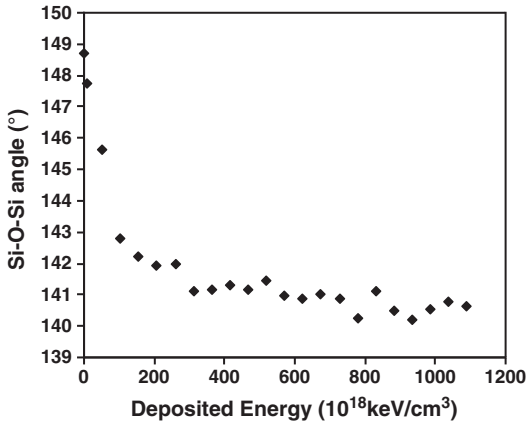

Fig. 11. Evolution of Si–O–Si angle in silica subjected to a series of 600 eV displacement cascades.

indicated by the broader distribution of the Si–O and O–O peaks on the radial distribution functions (Fig. 13).

4. Discussion

Numerical simulations show striking similarities and differences between the behavior of silica and CJ1 glasses as a result of ballistic collisions. In both cases, the glass structure undergoes an increase in the degree of disorder resulting in a broadening of the atomic pair contributions in the radial distribution function and of the ring size distribution, a decrease in the T–O–T′ angles (where T and T′ are network formers), and an increase in the internal energy.

Ballistic effects modify the glass structure, which stabilizes in a less stable configuration. Ballistic effects are similar to the effects of thermal quenching. Temperature rises sharply for a short time at the center of the cascade, then the glass is rapidly quenched under the influence of the surrounding material at a room temperature. Quenching rates at the center of the cascade were estimated to be larger than 10^{15} K/s. The initial glass is gradually replaced by a glass quenched at a much higher rate, hence with the memory of a higher fictive temperature. The decrease of the T–O–T′ angle during irradiation in both silica and CJ1 glasses, regardless of material swelling or densification, has different origins. In silica, the formation of SiO_5 or even SiO_6 sites and of oxygen triclusters results in a decrease in the mean value of the Si–O–Si angle. In CJ1 glass, this decrease is primary due to the B coordination change. The higher concentration of network modifying Na, presenting short Na–O distances, result in an overall convergence between O and Na. This tends to shift the network formers away from the central oxygen atom, hence a decrease in the T–O–T′ angles. This mechanism had already been identified in [29] with regard to Si–O–Al and Si–O–Si angles in the presence of calcium.

Experiments and simulations at different quenching rates have qualitatively reproduced the effects of displacement cascades. Silica and CJ1 glasses exhibit different behavior in terms of swelling and coordination number variations. In silica, the density increases together with the local coordination numbers. This structural change has been shown during polyamorphic transformations of SiO_2 or GeO_2 glasses at high pressure [30,31]. By contrast, in the CJ1 glass, the swelling corresponds to structural modifications usually observed at a high temperature, with a decrease in the boron coordination number and a modification of the role of Na^+ ions. The complex interplay between these two processes may explain the large variability of the volume changes of nuclear glasses during irradiation and indicates a strong chemical dependence of these macroscopic properties during glass irradiation [2].

5. Conclusion

MD simulations of a series of displacement cascades in silica and in SiO_2–B_2O_3–Na_2O glasses entail a structural change reflecting increasing disorder in the glass and increasing internal energy. In both glasses the T–O–T′ angles (where T and T′ are network formers) diminish while the ternary glass swells and silica becomes denser, which shows that these two effects are not correlated. A local thermal quenching model is proposed to account for the effects of ballistic collisions. The core of a displacement cascade is heated by the passage

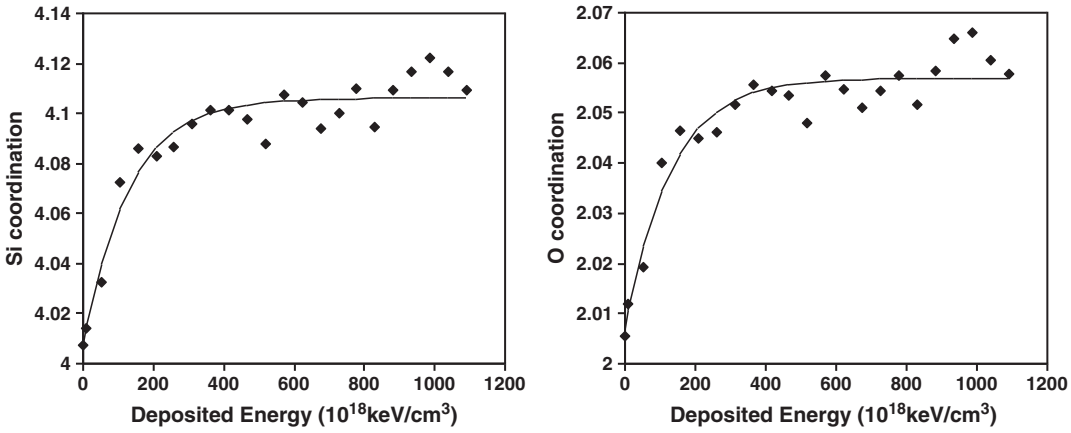

Fig. 10. Evolution of the coordination numbers of Si and O in silica subjected to a series of 600 eV displacement cascades.

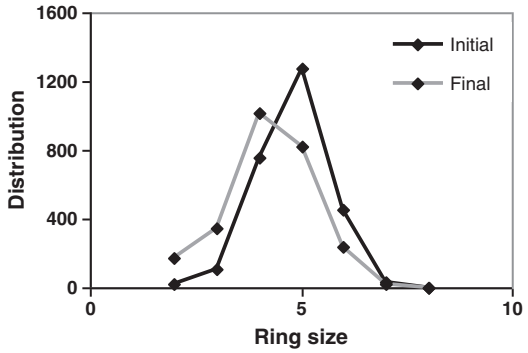

Fig. 12. Ring size distribution before and after the accumulation of a series of 600 eV cascades in silica.

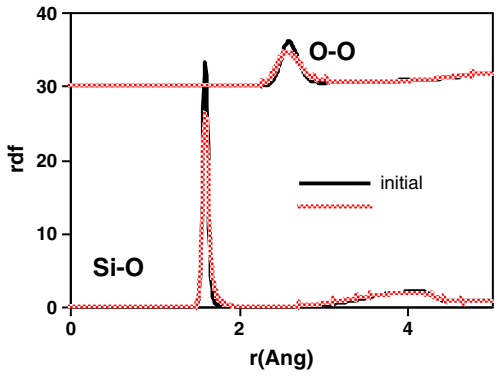

Fig. 13. Radial distribution functions for Si–O and O–O in silica before and after the accumulation of a series of 600 eV displacement cascades.

of a projectile, then rapidly quenched, leading to a process that mimics the effect of a local thermal quenching. The observed changes in both the mechanical and structural properties eventually reach saturation as the accumulated energy increases. The passage of a single projectile is sufficient locally to reach the maximum degree of damage, confirming the hypothesis postulated in the swelling model proposed by J.A.C. Marples.

Acknowledgments

We thank AREVA NC for financial support, and we gratefully acknowledge the CCRT for enabling these calculations.

References

[1] G. Calas, L. Galoisy, L. Cormier, J.-M. Delaye, P. Jollivet, S. Peuget, Mater. Res. Soc. Symp. Proc. 1265 (2010), 1265-AA03-01.
[2] W.J. Weber, R.C. Ewing, C.A. Angell, G.W. Arnold, A.N. Cormack, J.-M. Delaye, D.L. Griscom, L.W. Hobbs, A. Navrotsky, D.L. Price, A.M. Stoneham, M.C. Weinberg, J. Mater. Res. 12 (1997) 1946.
[3] Hj. Matzke, E. Vernaz, J. Nucl. Mater. 201 (1993) 295.
[4] M.T. Robinson, J. Nucl. Mater. 216 (1994) 1.
[5] S. Peuget, P.-Y. Noël, J.-L. Loubet, S. Pavan, P. Nivet, A. Chenet, Nucl. Instr. Meth. B 246 (2006) 379.
[6] S. Peuget, J.-N. Cachia, C. Jégou, X. Deschanels, D. Roudil, V. Broudic, J.-M. Delaye, J.-M. Bart, J. Nucl. Mater. 354 (2006) 1.
[7] J. de Bonfils, S. Peuget, G. Panczer, D. de Ligny, S. Henry, P.-Y. Noël, A. Chenet, B. Champagnon, J. Non-Cryst. Solids 356 (2010) 388.
[8] G. Bureau, J.-M. Delaye, S. Peuget, G. Calas, Nucl. Instr. Meth. B 266 (2008) 2707.
[9] W. Primak, Phys. Rev. 110 (1958) 1240.
[10] R.A.B. Devine, Nucl. Instr. Meth. B 91 (1994) 378.
[11] K. Moritani, Y. Teraoka, H. Moriyama, J. Nucl. Mater. 329 (2004) 998.
[12] G.W. Arnold, Radiat. Eff. Def. Solids 98 (1986) 55.
[13] G. Buscarino, S. Agnello, F.M. Gelardi, R. Boscaino, J. Phys. Condens. Matter 22 (2010) 255403.
[14] J.E. Shelby, J. Appl. Phys. 50 (1979) 3702.
[15] J.-M. Delaye, D. Ghaleb, Phys. Rev. B 61 (14) (2000) 481.
[16] J.-M. Delaye, D. Ghaleb, Nucl. Instr. Meth. B 250 (2006) 57.
[17] W.J. Dell, P.J. Bray, S.Z. Xiao, J. NonCryst. Solids 58 (1983) 1.
[18] L.S. Du, J.F. Stebbins, J. Phys. Chem. B 107 (2003) 10063.
[19] A. Grandjean, M. Malki, V. Montouillout, F. Debruycker, D. Massiot, J. NonCryst. Solids 354 (2008) 1664.
[20] F.H. Stillinger, T.A. Weber, Phys. Rev. B 31 (1985) 5262.
[21] B.W.H. Van Beest, G.J. Kramer, R.A. van Santen, Phys. Rev. Lett. 64 (1990) 1955.
[22] J.F. Ziegler, J.P. Biersack, U. Littmark, The Stopping Range of Ions in Matter, Pergamon, New York, 1985.
[23] J.-M. Delaye, D. Ghaleb, Phys. Rev. B 71 (224) (2005) 203.
[24] J.A.C. Marples, Nucl. Instr. Meth. B 32 (1988) 480.
[25] O. Majérus, L. Cormier, G. Calas, B. Beuneu, Phys. Rev. B 67 (2003) 024210.
[26] S. Ito, T. Taniguchi, J. Non-Cryst. Solids 349 (2004) 173.
[27] C. Levelut, R. Le Parc, A. Faivre, B. Champagnon, J. Non-Cryst. Solids 352 (2006) 4495.
[28] J.F. Stebbins, S.E. Ellsworth, J. Am. Ceram. Soc. 79 (1996) 2247.
[29] F. Angeli, J.-M. Delaye, T. Charpentier, J.-C. Petit, D. Ghaleb, P. Faucon, Chem. Phys. Lett. 320 (2000) 681.
[30] J.P. Itie, A. Polian, G. Calas, J. Petiau, A. Fontaine, H. Talentino, Phys. Rev. Lett. 63 (1989) 398.
[31] O. Majerus, L. Cormier, J.P. Itie, L. Galoisy, D.R. Neuville, G. Calas, J. Non-Cryst. Solids 345–346 (2004) 34.